



# Anticarcinogenic trimethoxybenzoate of catechin stabilizes the liquid crystalline bilayer phase in phosphatidylethanolamine membranes



Elisa Aranda<sup>a,1</sup>, José A. Teruel<sup>a</sup>, Antonio Ortiz<sup>a</sup>, María Dolores Pérez-Cárceles<sup>b</sup>, José N. Rodríguez-López<sup>a</sup>, Francisco J. Aranda<sup>a,\*</sup>

<sup>a</sup>Departamento de Bioquímica y Biología Molecular A, Universidad de Murcia, 30100 Murcia, Spain

<sup>b</sup>Departamento de Medicina Legal y Forense, Facultad de Medicina, Instituto de Investigación Biomédica (IMIB Arrixaca), Universidad de Murcia, 30120 Murcia, Spain

## ARTICLE INFO

### Article history:

Received 28 June 2022

Revised 29 September 2022

Accepted 6 November 2022

Available online 11 November 2022

### Keywords:

Catechin

Dielaidoylphosphatidylethanolamine

Phospholipid membrane

Lipid polymorphism

## ABSTRACT

The anticarcinogenic properties of catechins stand out among the great variety of biological actions attributed to these compounds. The capacity of catechins to interact with lipids and their participation in membrane related processes points out to the membrane as their potential site of action. Phosphatidylethanolamine is an abundant phospholipid in mammalian membranes that has tendency to form non lamellar phases, it is associated with important cellular processes, and it has been related to cancer. In order to shed light into the molecular effect of the anticarcinogenic 3,4,5-trimethoxybenzoate of catechin (TMBC) on lipid polymorphism and membrane structure and dynamics, we present a combined experimental and computational study of the interaction between this semisynthetic catechin and biomimetic membranes composed of unsaturated phosphatidylethanolamine. Our experimental evidence reveals that TMBC is readily incorporated into unsaturated phosphatidylethanolamine system where it is able to shift the gel to liquid crystalline phase transition temperature to lower values, decreasing the cooperativity and the enthalpy change of the transition. The presence of TMBC is able to promote the formation of gel phase immiscibility and to block the formation of the inverted hexagonal phase. In the bilayer liquid crystalline phase, the catechin decreases the interlamellar repeat distance, it increases the fluidity of the membrane, and it alters the hydrogen bond pattern of the interfacial region of the bilayer. Our molecular dynamics results concur with the experimental data and locate TMBC forming different domains near the interfacial region of the bilayer where it modifies the lateral pressure profile of the membrane leading to a stabilization of the bilayer in the liquid crystalline phase and to a potential alteration of the function of the membrane.

© 2022 The Author(s). Published by Elsevier B.V. This is an open access article under the CC BY-NC-ND license (<http://creativecommons.org/licenses/by-nc-nd/4.0/>).

## 1. Introduction

A considerable number of studies have established that green tea catechins have healthful effects on many human disorders, among other things obesity, metabolic syndrome, neurodegenera-

tive and inflammatory diseases, and also cancer [1]. Regarding the important beneficial effects on cancer in humans, catechins exhibit hopeful results in a considerable number of different cancers [2], and most of the anticancer effects of catechins are performed fundamentally through the interaction between catechins and a variety of membrane proteins, intracellular targets, and also the plasma membrane itself [3].

The membrane has emerged as a probable place for the anticancer task of catechins and there are evidences that catechins interact with phospholipid bilayers [4], changing the stiffness of the membrane and affecting lipid rafts [5–7]. For that reason, the interaction of catechins with the membrane is very important to shed light into their mechanism of action, however, the study of this interaction is arduous as the composition of membranes is very complex. The existence of different kind of lipids is outstand-

**Abbreviations:** DEPE, 1,2-Dielaidoyl-*sn*-glycero-3-phosphoethanolamine; DSC, Differential scanning calorimetry; FTIR, Fourier transform infrared spectroscopy; HII, Inverted hexagonal phase; L $\beta$ , Normal gel phase; L $\alpha$ , Liquid crystalline phase; SAXD, Small angle X-ray diffraction; TMBC, 3,4,5-Trimethoxybenzoate of catechin; WAXD, Wide angle X-ray diffraction.

\* Corresponding author.

**E-mail addresses:** [elisa.aranda@um.es](mailto:elisa.aranda@um.es) (E. Aranda), [teruel@um.es](mailto:teruel@um.es) (J.A. Teruel), [ortizbq@um.es](mailto:ortizbq@um.es) (A. Ortiz), [mdperez@um.es](mailto:mdperez@um.es) (M. Dolores Pérez-Cárceles), [neptuno@um.es](mailto:neptuno@um.es) (J.N. Rodríguez-López), [fjam@um.es](mailto:fjam@um.es) (F.J. Aranda).

<sup>1</sup> Present Address: Hospital Universitario Virgen de la Arrixaca, Área de Salud 1, 30120 Murcia, Spain.

<https://doi.org/10.1016/j.molliq.2022.120774>

0167-7322/© 2022 The Author(s). Published by Elsevier B.V.

This is an open access article under the CC BY-NC-ND license (<http://creativecommons.org/licenses/by-nc-nd/4.0/>).

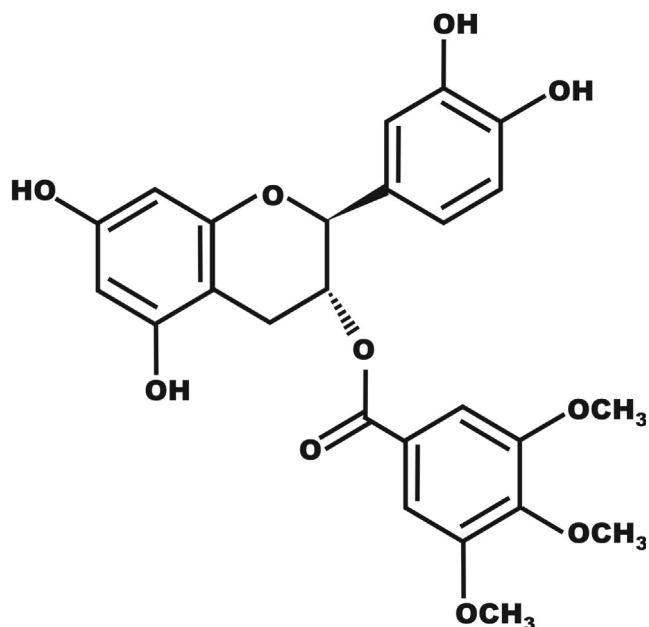


Fig. 1. Chemical structure of TMBC.

ing because they confer the distinct membranes with special properties regarding permeability, fluidity or thickness [8].

Phosphatidylethanolamine is the second most abundant phospholipid on mammalian cellular membranes, its presence reaching nearly 30 % of total phospholipids [9], most of which is asymmetrically distributed in the inner leaflet of the membrane. Phosphatidylethanolamine has been shown to be associated with protein biogenesis and activity, oxidative phosphorylation, autophagy, membrane fusion, mitochondrial stability, and it is an important precursor of other lipids [10]. Phosphatidylethanolamine contains a small polar head group and when combined with the presence of unsaturated fatty acyl chains is capable of forming non-bilayer phases [11]. The inherent negative spontaneous curvature of this cone-shaped lipid has the tendency to generate hexagonal inverted phases inside the membrane, which promote different membrane events involving the generation of non-bilayer membrane intermediates, like in fusion [12], the integration of proteins into membranes and the modulation of conformational changes in protein structure [13].

It is interesting that phosphatidylethanolamine has been shown to increase its presence on the outer membrane of tumor vascular endothelium cells, suggesting that it may serve as a marker for tumor vasculature and also drug targeting [14]. This feature, as well as a high degree of expression of phosphatidylethanolamine on endothelial cells in tumor vasculature, makes phosphatidylethanolamine an attractive molecular target for future cancer interventions [15]. There are several reports which show the relation between phosphatidylethanolamine and cancer, among them, the demonstration that the anticancer and toxic properties of cyclotides are dependent on phosphatidylethanolamine targeting [16], the conclusion that the potent anticancer activity of the sesterterpenoid Ophioboliln A is also targeted to phosphatidylethanolamine [17], and the evidence that the tumor suppressor LACTB acts decreasing the presence of phosphatidylethanolamine in the membrane [18]. It is apparent that the study of the interaction between catechins and unsaturated phosphatidylethanolamine would be crucial to understand the effects of these compounds on the membrane.

New catechin derivatives have been developed to overcome the restrictions of use of catechins presented by their low stability in

neutral solutions and their inability to readily cross cellular membranes [19]. TMBC (Fig. 1) is a modified catechin that has demonstrated to exhibit a high activity against melanoma and breast cancer cells [20,21], and which has been shown to perturb the structural properties of important zwitterionic [22,23] and anionic phospholipids [24]. The main objective of this work is to study at molecular level the effect of TMBC on lipid polymorphism, an important question not investigated so far. In particular, we investigate the influence of TMBC on the propensity of phosphatidylethanolamines to form non bilayer phases. We have used several experimental techniques, including differential scanning calorimetry (DSC), X-ray diffraction, and Fourier transform infrared (FTIR) spectroscopy, together with molecular dynamics simulation, to study the interaction between TMBC and model membrane systems composed by 1,2-dielaidoyl-*sn*-glycero-3-phosphoethanolamine (DEPE). We have chosen DEPE because it is a phospholipid that undergoes transitions from gel to liquid crystalline and from bilayer to inverted hexagonal phases in a range of temperatures that can be studied using the appropriate techniques. We believe that the obtained information will contribute to advance on the understanding of the molecular interaction between the semisynthetic catechin and the membrane.

## 2. Materials and methods

### 2.1. Materials

DEPE (>99 % TLC) was purchased from Avanti Polar Lipids Inc. (Birmingham, AL), and phosphorous analysis was used to determine phospholipid concentration [25]. (–)-Catechin and 3,4,5-trimethoxybenzoyl chloride were purchased from Sigma Chemical Co. (Madrid, Spain), and TMBC was synthesized from catechin as detailed previously [20]. All other reagents were of the highest purity obtainable.

### 2.2. Differential scanning calorimetry

Samples for DSC were prepared by drying organic solvent solutions containing convenient quantities of DEPE and TMBC, and forming multilamellar vesicles in 150 mM NaCl, 0.1 mM EDTA, 10 mM Hepes, pH 7.4 buffer, essentially as described in [22]. Samples were measured in a MicroCal PEAQ-DSC calorimeter (Malvern Panalytical, Malvern, UK) at 1.5 mM final phospholipid concentration, and heating scan rate of 60 °C h<sup>-1</sup>. Data were studied using ORIGIN v7.0383 (Northampton, MA, USA). Areas under the thermograms were used to determine the enthalpy change of the transitions, and onset and completion temperatures were used to construct a partial phase diagram, after correction by the finite width of the transitions of pure DEPE.

### 2.3. X-ray diffraction

Samples containing 10 μmol of DEPE and convenient amount of TMBC, prepared similarly as those described for DSC, were centrifuged 5 min at 12000 rpm. Pellets were placed in a steel holder and were measured in a modified Kratky compact camera (MBraun-Graz-Optical Systems, Graz, Austria). Nickel-filtered Cu K $\alpha$  X-rays were generated by a Philips PW3830 X-ray Generator operating at 50 kV and 30 mA. The  $q$  (scattering vector) range covered ( $q = 4\pi \sin \theta / \lambda$ ; where  $2\theta$  is the scattering angle and  $\lambda = 1.54 \text{ \AA}$  the selected X-ray wavelength) was between 0.05 and 0.6  $\text{\AA}^{-1}$  for small angle X-ray diffraction (SAXD), and from 1.32 to 1.95  $\text{\AA}^{-1}$  for wide angle X-ray diffraction (WAXD). SAXD and WAXD were accomplished at the same time essentially as described previously [22].

## 2.4. FTIR spectroscopy

Samples for the infrared measurements containing 10  $\mu\text{mol}$  of DEPE and convenient amount of TMBC were formed in 75  $\mu\text{L}$  of the same buffer prepared in  $\text{D}_2\text{O}$  as described above. Infrared spectra were collected in a Nicolet 6700 FTIR spectrometer (Thermo Fisher Scientific, Madison, WI, USA) essentially as described previously [22]. Spectra were analyzed using the software Grams (Galactic Industries, Salem, NH, USA).

## 2.5. Molecular dynamics

The molecular structure of TMBC was constructed from the chemical structure of (-)-Catechin gallate obtained from the Pub Chem Substance and Compound data base [26] through the identifier number 6419835. All molecular dynamics simulations were done using GROMACS 5.0.7 and 2018.1 [27] with the aid of the Computational Service of the University of Murcia (Spain).

CHARMM36 force field parameters for dioleoylphosphatidylethanolamine, TMBC, water,  $\text{Cl}^-$  and  $\text{Na}^+$  were obtained from CHARMM-GUI [28–30]. DEPE topology file was built from dioleoylphosphatidylethanolamine force field parameters changing the dihedral restraints from the cis to the trans double bond.

Packmol software [31] was used to build the initial membrane structures formed by 2 leaflets oriented normal to the z-axis. The bilayer membrane was built with 128 molecules of DEPE with and without 14 molecules of TMBC, with a water layer containing a total of 6400 water molecules (TIP3 model), 144 sodium ions, and 144 chloride ions. DEPE and TMBC were randomly distributed in each phospholipid layer keeping the DEPE molecules oriented normal to z-x plane, and thus in the different simulations the TMBC molecules were at different random starting locations in the lipid phase. All systems were simulated using the NpT-ensemble at 50 °C constant average temperature. Pressure was controlled semi-isotropically at 1 bar of pressure and  $4.5 \times 10^{-5} \text{ bar}^{-1}$  of compressibility. The cutoffs for van der Waals and short-range electrostatic interactions were set to 1.2 nm, and a force switch function was applied between 1.0 and 1.2 nm. Equilibration was undertaken for 3 ns using the V-rescale temperature coupling method, and Berendsen pressure coupling method [32]. Equilibration was followed by production runs of 300 ns using the Nose-Hoover thermostat [33] and the Parrinello-Rahman barostat [34].

Graphical representation and inspection of all molecular structures were done with PyMOL 2.3.0 [35]. The last 40 ns of the production run were used for the analysis by using Gromacs tools.

To calculate the lateral pressure profile  $\pi(z)$  we used GROMACS-LS [36–39], a custom version of GROMACS that allows the calculation of the local stress tensor in three dimensions. Rerun of the last 100 ns simulated trajectories was necessary to output the local stress tensors using an increased cutoff distance of 2.2 nm for Coulomb interactions as recommended by the software package authors. The simulation box was divided into 1 Å thick slabs normal to the z-axis. For a slab centered at depth z, the lateral pressure profile  $\pi(z)$  is defined as:

$$\pi(z) = \frac{P_{xx}(z) - P_{yy}(z)}{2} - P_{zz}(z)$$

where  $P_{xx}(z)$ ,  $P_{yy}(z)$  and  $P_{zz}(z)$  are the diagonal elements of the pressure tensor, along the x, y and z axes, respectively [38]. All the profiles were smoothed by a spline function and symmetrized with respect to the bilayer center.

## 3. Results and discussion

### 3.1. Differential scanning calorimetry

We used DSC to investigate the effect of TMBC on the DEPE thermotropic behavior. Fig. 2A shows the heating thermograms of DEPE dispersions and mixtures of DEPE and TMBC. Pure DEPE shows two endotherms, a major peak at 37 °C and a minor peak at 63.7 °C, which correlate with the bilayer  $\text{L}\beta$  to bilayer  $\text{L}\alpha$  phase transition and to the bilayer to  $\text{H}_{\text{II}}$  phase transition respectively, in agreement with previous reports [40,41]. When TMBC is incorporated into DEPE in a low catechin mole fraction like 0.02, the main chain melting transition is already clearly affected as the temperature of the onset of the melting transition is shifted to lower values and the transition is wider. This trend is kept when more TMBC is present in the system, and when the mole fraction of TMBC is higher than 0.15 the main transition is distinctly composed by two broad components.

An interesting finding is the appearance of a cooperative endotherm at a constant onset temperature of 22 °C, this peak is already present at low mole fraction of TMBC, and it became more evident as the concentration of TMBC is increased, its size increasing at the expenses of the main higher melting endotherm. The presence of an additional endotherm at a lower invariable temperature has been previously reported in mixtures of TMBC and shorter saturated phosphatidylethanolamine [23]. DSC results suggest that TMBC is readily incorporated into DEPE system where it can interact with the phospholipid acyl chains, affecting their structural properties and producing that the melting transition is less cooperative and shifted to lower temperatures. It can be observed in Fig. 2B that the perturbation exerted by TMBC on the acyl chains of DEPE produces that the enthalpy change of the melting transition decreases as more TMBC is present into the system.

The presence of different broad components in the main transition may point out that different domains are present in the bilayer, and the presence of a lower temperature component at a fixed temperature suggests the formation of a stable component or a different phase. As shown in Fig. 2C, the effect of TMBC on the lamellar to  $\text{H}_{\text{II}}$  phase transition of DEPE is also evident, the presence of increasing concentrations of the catechin produces a broadening and shifting of the transition endotherm to higher temperatures.

### 3.2. X-ray diffraction

Information of structural characteristics of the TMBC/DEPE system was acquired by using SAXD and WAXD. We registered the diffractions profiles of TMBC/DEPE samples at different temperatures, and the results are presented in Fig. 3. The SAXD technique allows to designate the macroscopic structure of the system, and also to determine the interbilayer repeat distance in the bilayer phase and the tube diameter in the  $\text{H}_{\text{II}}$  phase. When phospholipid organized themselves into multilamellar structures, they give rise to several reflections which distances relate as 1: 1/2: 1/3: 1/4 ... [42]. It can be seen from the SAXD patterns presented in Fig. 3A that pure DEPE at 15 °C, i.e., below the  $\text{L}\beta$  to  $\text{L}\alpha$  phase transition, shows a first order reflection at 66.3 Å, this first order reflection correlates with the interbilayer repeat distance, which includes the bilayer thickness and the layer of water between bilayers, and agrees with previous reports [43,44]. It has been previously shown that DEPE systems in the lamellar phase do not show higher order reflections [41,45], however, we can detect a sharp reflection near 16.5 Å, which corresponds to the fourth order reflection appearing at 1/4 the distance relative to the observed first order reflection. At 15 °C, the presence of TMBC does not alter the dis-

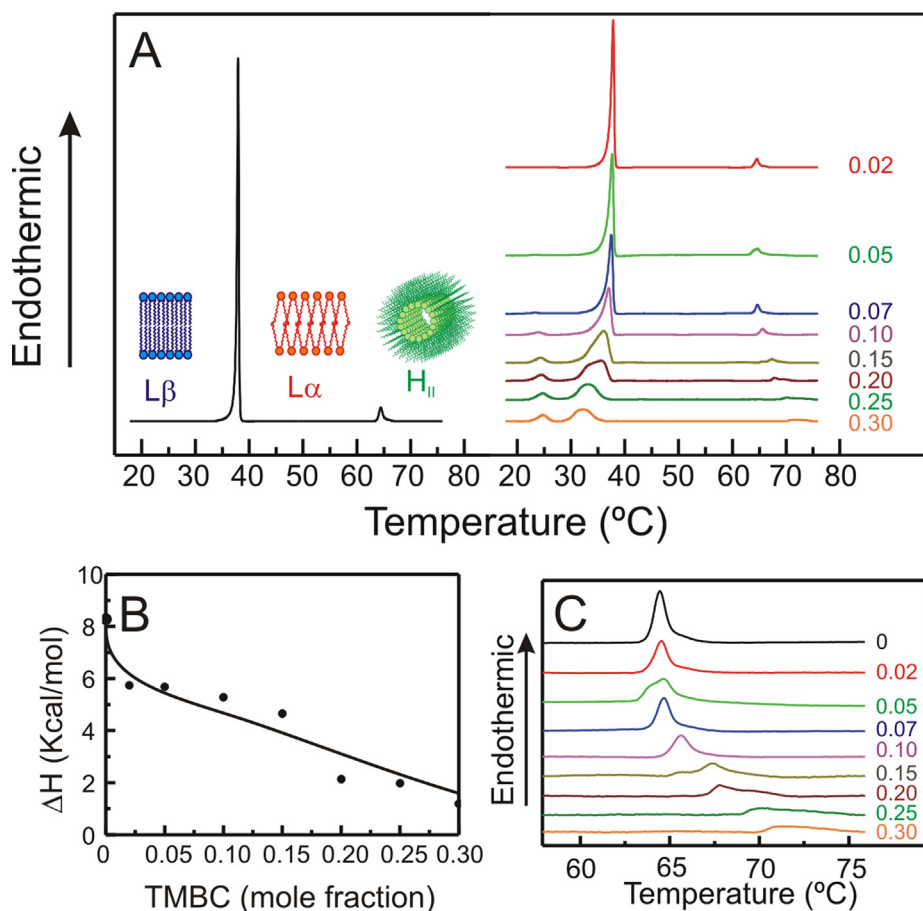


**Fig. 2.** (A) DSC heating thermograms for pure DEPE (left) and DEPE containing TMBC at different concentrations (right). (B) Enthalpy change for the bilayer L $\beta$  to L $\alpha$  phase transition. (C) Enlargement of the bilayer to H $_{II}$  transition region of the thermograms. TMBC mole fractions are expressed on the right side of the thermograms.

tance of the first order reflection, but in the case of 0.07 mol fraction a weak third order reflection could also be observed. The WAXD technique supplies data correlating to the packing of the phospholipid acyl chains. Fig. 3B shows that at 15 °C, all the systems display a symmetric sharp reflection centered at 4.2 Å, conclusive of the usual L $\beta$  phase, where the acyl chains adopt regular hexagonal lattice parallel to the bilayer normal.

At 28 °C, pure DEPE is still organized in the L $\beta$  phase, but increasing the temperature at 50 °C, i.e., above the main L $\beta$  to L $\alpha$  phase transition, the first order distance decreases to 53.7 Å, and with second, third and fourth order reflections being also weakly detected (Fig. 3A). This dramatic reduction in the first order repeat distance is due to the decrease in the effective acyl chain length which goes with the transition to the L $\alpha$  phase, and it is corroborated by the broad diffuse dispersion characteristic of this phase found in the WAXD region at 50 °C (Fig. 3B). However, at 28 °C, in the presence of 0.07 mol fraction of TMBC weak additional reflections appear at 51.9 and 25.4 Å, reflections which are sharper and more apparent in the presence of 0.20 mol fraction of TMBC (Fig. 3A). These additional reflections correspond to the first and second reflections of a L $\alpha$  phase, which is present simultaneously with the more abundant L $\beta$  phase. The sharp reflection corresponding to the L $\beta$  phase is the only one detected in the WAXD region (Fig. 3B), as the L $\alpha$  phase produces diffuse scattering pattern. The L $\alpha$  phase detected at 28 °C corresponds to the phospholipids that in the presence of TMBC undergo the L $\beta$  to L $\alpha$  phase transition at lower temperatures, which gave rise to the invariable low temperature endotherm detected by DSC (Fig. 2A).

At 50 °C, pure DEPE and TMBC/DEPE systems are organized in the bilayer L $\alpha$  phase, as seen by the diffuse scattering pattern observed by WAXD (Fig. 3B) and the four reflections relating as 1: 1/2: 1/3: 1/4 characteristic of the bilayer organization (Fig. 3A). Nevertheless, it is interesting to note that the first order distance in the L $\alpha$  phase observed at 53.7 Å for pure DEPE, decreases to 52.9 Å in the presence of 0.07 mol fraction of TMBC, and to 51.2 Å in the presence of 0.20 mol fraction of TMBC. The latter indicates that the incorporation of TMBC in the L $\alpha$  phase of DEPE decreases the interlamellar repeat distance of the system, which is congruent with the reduction in the bilayer thickness reported previously for the presence of TMBC in zwitterionic and anionic phospholipid membranes [22–24].

When phospholipids organize themselves in hexagonal H $_{II}$  structures they generate SAXD reflections which distances relate as 1: 1/ $\sqrt{3}$ : 1/ $\sqrt{4}$ : 1/ $\sqrt{7}$  ... [42]. Pure DEPE at 66 °C produces a first order reflection at a distance of 64.1 Å and the corresponding second, third and fourth reflections with distances characteristic of the H $_{II}$  phase (Fig. 3A). The characteristic WAXD diffuse pattern of DEPE at 66 °C indicates the fluid nature of the H $_{II}$  phase (Fig. 3B). In the presence of 0.07 mol fraction of TMBC, the system presents the characteristic reflections of the H $_{II}$  phase, but a weak reflection at a distance of 50.8 Å is also present (Fig. 3A) which indicates the presence of a minor portion of the phospholipid that are still organized in the bilayer L $\alpha$  phase. Interestingly, in the presence of 0.20 mol fraction of TMBC the reflection pattern characteristic of the H $_{II}$  phase is not found and it is replaced by three order reflections related as 1: 1/2: 1/3 characteristic of the L $\alpha$

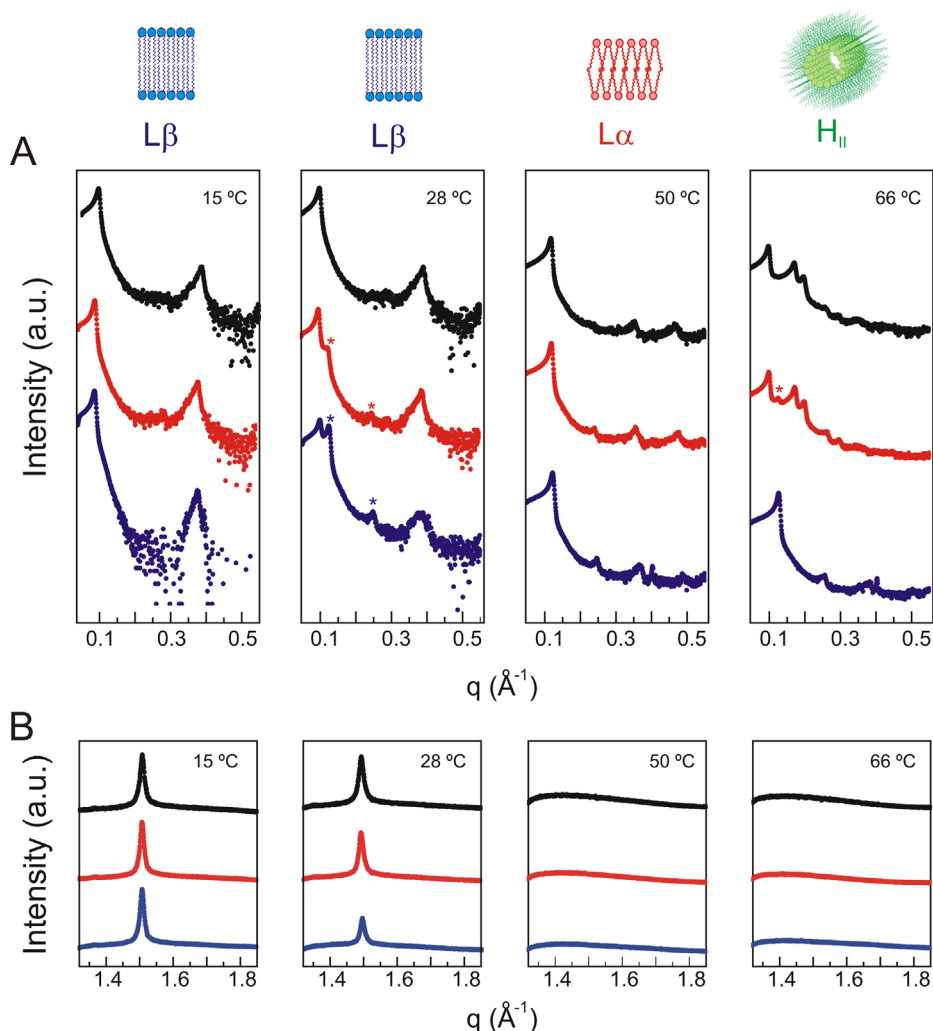


**Fig. 3.** (A) Intensity (log scale arbitrary units) vs scattering vector ( $q$ ) for SAXD profiles of pure DEPE (top black), DEPE containing TMBC 0.07 (middle red) and 0.20 mol fraction (bottom blue) at different temperatures. The asterisks indicate reflections arising from a bilayer  $L\alpha$  phase in mixture with another phase. (B) Intensity (arbitrary units) vs scattering vector ( $q$ ) for WAXD profiles of pure DEPE (top black), DEPE containing TMBC 0.07 (middle red) and 0.20 mol fraction (bottom blue) at different temperatures.

phase, with a further decreased interbilayer repeat distance of 49 Å. The latter reveals the role of TMBC as an important stabilizer of this phase. The diameter of the tubules which form the hexagonal array of the  $H_{II}$  phase can be determined by multiplying by two the distance of the second order reflection of the hexagonal  $H_{II}$  SAXD pattern [46], in the case of pure DEPE we found a tube diameter of 73.6 Å, and this value did not change by the presence of TMBC.

From the DSC thermograms showed in Fig. 2A, we determined the onset and completion temperatures of the different endothermic transitions. When these data were put together with the structural information obtained from the X-ray experiments, they allowed us to construct the partial phase diagram for DEPE in mixtures with TMBC presented in Fig. 4. It can be observed that the temperature of the solidus and fluidus lines, that is, the boundary lines formed with the onset and completion temperatures of the main  $L\beta$  to  $L\alpha$  phase transition (circles in Fig. 4), decreases as more TMBC is present in the system, and this indicates a near ideal mixing behaviour, that is, good miscibility in both phases. However, as commented above (Fig. 2A), as soon as the TMBC concentration is increased, the phase diagram is dominated by a clear gel phase immiscibility. Below 22 °C, there are two different  $L\beta$  phases: a minor  $L\beta_1$  phase, which appears to have a fixed stoichiometry

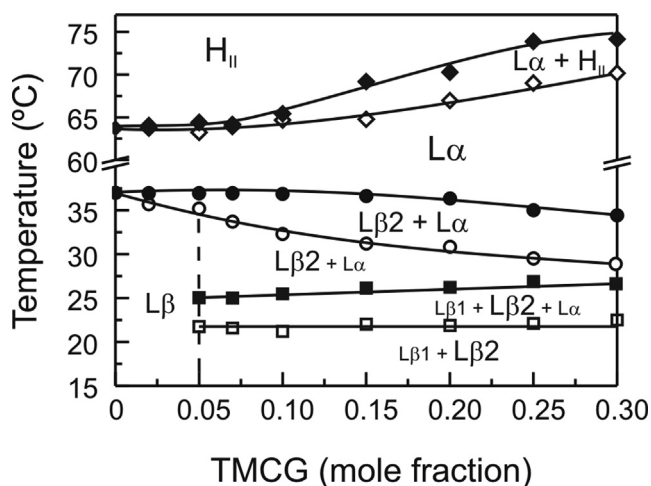


**Fig. 4.** Partial phase diagram for DEPE in DEPE/TMBC mixtures. Open and solid symbols were obtained from the onset and completion temperatures of the bilayer  $L\beta$  to  $L\alpha$  (squares and circles) and the bilayer to  $H_{II}$  phase transitions (diamonds), after correction by the finite width of the transitions of pure DEPE.

and a transition temperature that does not change as more TMBC is present in the membrane; and a major  $L\beta_2$  phase, in which TMBC is miscible with DEPE, and which shows a transition temperature that is higher than that of  $L\beta_1$ , and decreases as more TMBC is present in the membrane. The system then evolves from an immiscible gel phase to a phase in which there is a coexistence of a  $L\beta_2$  phase, and a  $L\alpha$  phase from the melting of the  $L\beta_1$  phase, and then to a region of  $L\alpha$  phase in which all the phospholipids are organized in the bilayer liquid crystalline phase. Finally, the hexagonal boundary lines show good miscibility as their temperatures increase as more TMBC is present in the membrane, and the phospholipid evolves from the  $L\alpha$  phase to the  $H_{II}$  phase through a region of coexistence which is wider as more TMBC is present. Interestingly, the increase of the temperature of the hexagonal boundaries conduces to a stabilization of the region of liquid crystalline bilayer which occupy a wider region in the phase diagram.

It is interesting to note that, in our DEPE system, this immiscibility appears at a very low concentration of TMBC (0.05 mol fraction), but in the case of dimyristoylphosphatidylethanolamine it was shown to require the presence of considerable higher amounts of TMBC (0.20 mol fraction) to be observable [23]. The latter might be due to a higher miscibility of TMBC in the shorter phosphatidylethanolamine acyl chain homologue. For the antitumor compound paclitaxel, it has been shown that the lipid chain length influences drug membrane interactions. Phospholipids of shorter chain length have a higher ability to incorporate the antitumor compound, while longer chains prevent the incorporation process due to stronger van der Waals forces and higher packing [47]. This is in line with the general observation that the incorporation of amphiphilic molecules into the interior of membranes decreases as a function of the chain length [48].

### 3.3. FTIR spectroscopy

We carried out FTIR spectroscopy experiments to sense the perturbation exerted by TMBC on different part of DEPE molecule. The two most informative absorption regions are the methylene and the carbonyl stretching bands, which account respectively for the properties of the acyl chains and the interfacial regions of the phospholipid molecule.

Fig. 5 presents the position of the maximum of the infrared symmetric methylene stretching band,  $\nu_s\text{CH}_2$ , which corresponds to pure DEPE and DEPE/TMBC mixtures as a function of the temperature. Pure DEPE in the  $L\beta$  phase shows absorbance maximum near  $2848.5\text{ cm}^{-1}$ , this value increases to around  $2850\text{ cm}^{-1}$  after the transition to the  $L\alpha$  phase. This shift of the band maximum to higher values comes from the increment in the conformational disorder of the acyl chain that takes place during the melting phase transition due to the presence of higher proportion of gauche conformers [49]. A second less pronounced increase of the band maximum takes place when the phospholipid undergoes the bilayer to  $H_{II}$  phase transition, which implies that additional conformational disorder is introduced by this transition, in accordance to previous works [43,50]. The presence of TMBC has two clear consequences on the methylene absorption band of DEPE, first it produces that the  $L\beta$  to  $L\alpha$  phase transition is shifted to lower temperatures, this is in accordance with the DSC experiments (Fig. 2A), and second, the values of the wavenumber of the maximum of the band in the  $L\alpha$  phase appears at higher values when the concentration of TMBC is increased. The latter indicates that the acyl chains of DEPE are more disordered in the presence of TMBC, probably due to an increment of the proportion of gauche conformers. This increase in the acyl chain disorder is at difference to what has been reported for TMBC in dimyristoylphosphatidylserine bilayer where no effect in the maximum of the methylene band was observed in the  $L\alpha$  phase [24]. The stronger effect of TMBC on DEPE bilayers when

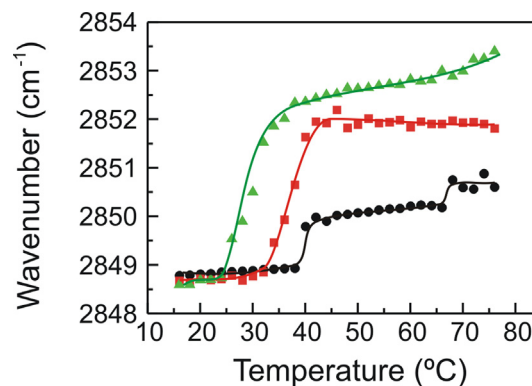


Fig. 5. Temperature dependence of the position of the maximum of the symmetric methylene stretching vibration band,  $\nu_s\text{CH}_2$ , exhibited by pure DEPE (black circles) and DEPE containing TMBC at 0.07 (red squares) and 0.20 (green triangles) mole fraction.

compared with that of dimyristoylphosphatidylserine might be due to a different location of the catechin in each phospholipid bilayer. It seems that in DEPE bilayers TMBC should be located in a place that enables it to exert a stronger perturbation on the acyl chains. This will be further discussed later, when mass density profiles along the bilayer normal are presented.

Fig. 6 presents the infrared spectra of the carbonyl stretching absorption band,  $\nu\text{C}=\text{O}$ , of DEPE and DEPE/TMBC mixtures at different temperatures. Pure DEPE in the  $L\beta$  phase (Fig. 6A) shows the maximum of the band near  $1738\text{ cm}^{-1}$ , this wavenumber decreases to near  $1732\text{ cm}^{-1}$  in the  $L\alpha$  phase (Fig. 6B), and then increases again to  $1734\text{ cm}^{-1}$  in the  $H_{II}$  phase (Fig. 6C). As seen in Fig. 6, the contour of the carbonyl stretching band is broad and asymmetric, suggesting that the band is composed of several components. It is known that this band is probably a composite of at least three components with maxima appearing at  $1742$ ,  $1728$ , and  $1714\text{ cm}^{-1}$ . It has been suggested that the band near  $1742\text{ cm}^{-1}$  emerges from a population of non-hydrogen bonded ester carbonyl groups, and that the bands near  $1728$  and  $1714\text{ cm}^{-1}$  emerge from carbonyl groups populations hydrogen bonded to water and amine group respectively [51,52]. In this way, when DEPE undergoes its  $L\beta$  to  $L\alpha$  phase transition, the observed decrease in the wavenumber is due to the enlargement of the lower wavenumber components at the expenses of the higher wavenumber component, and it is coherent with the increase in hydration that distinguish the bilayer  $L\alpha$  phase [50]. As it has been previously shown, the increase in wavenumber of the maximum of the carbonyl band observed when DEPE undergoes the bilayer to  $H_{II}$  phase transition, indicates that during the formation of the  $H_{II}$  phase a partial dehydration is produced [53,54]. In the presence of TMBC, the hydrogen bond availability may expand as there is the possibility of new hydrogen bonds between the carbonyl group of DEPE and the hydroxyl groups of TMBC, and also between the carbonyl group of TMBC and water. As seen in Fig. 6, in the presence of TMBC, the maximum of the carbonyl absorption band is shifted to lower wavenumbers, and this suggests, that at all the temperatures studied, the catechin affects the interfacial portion of the phospholipid and alters the hydrogen bond pattern of this region.

### 3.4. Molecular dynamics

We used computer molecular dynamics simulation to obtain atomic detail of the DEPE/TMBC system. The area per lipid at the membrane aqueous interface was calculated from the lateral

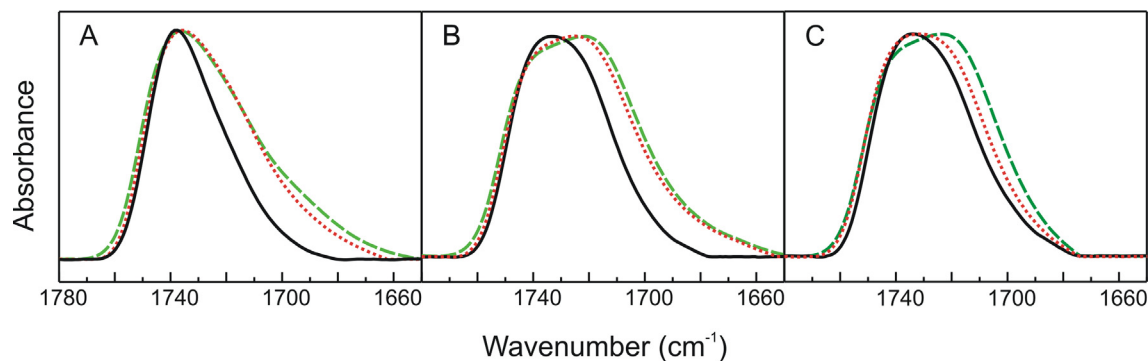


**Fig. 6.** FTIR ester carbonyl absorption band,  $\nu\text{C}=\text{O}$ , for pure DEPE (solid black lines), and DEPE containing TMBC at 0.07 (dotted red lines) and 0.20 (dashed green lines) mole fraction, at different temperatures: (A) 20 °C, (B) 50 °C, and (C) 72 °C.

dimensions of the simulation box (the area of the  $xy$  plane) divided by the number of lipids in each leaflet. We found that the area per lipid of the DEPE system in the bilayer  $L\alpha$  phase was  $0.59\text{ nm}^2$ , and that this value increased to  $0.64\text{ nm}^2$  in the presence of TMBC.

To obtain information regarding the fluidity of the bilayer we measured the *gauche/trans* conformer ratio. We found that this ratio increased from 0.54 for pure DEPE to 0.56 in the presence of TMBC. We also determined the order parameter of the bilayer, and we detected that this parameter decreased from 0.18 for pure DEPE to 0.16 in the presence of TMBC. These data indicate that the presence of TMBC increases the fluidity and decreases the order of the bilayer  $L\alpha$  phase of DEPE, and this is in agreement with the increase in fluidity as determined by the analysis of the infrared methylene absorption band of the system (Fig. 5).

Membrane thickness was determined from the distance between the averaged  $z$ -position of the phosphorous atoms of opposing leaflets. The membrane thickness obtained for the pure DEPE bilayer was  $42.6\text{ \AA}$ , and this distance decreased to  $40.9\text{ \AA}$  in the presence of TMBC. This measurement is in agreement with the decrease in the interlamellar repeat distance detected by SAXD in the presence of TMBC (Fig. 3B). This reduction of the membrane thickness exerted by TMBC is of significance because it might affect the hydrophobic mismatch between the hydrophobic length of integral proteins and the hydrophobic part of the bilayer [55], and it could cause alteration in the structure and function of proteins [56].

In order to include both strong and moderate hydrogen bonds we assumed hydrogen bond formation when the distance between hydrogen donor and the DEPE carbonyl was shorter or equal to  $3\text{ \AA}$  and the H-bond angle was less than or equal to  $30^\circ$ . The analysis of the carbonyl interactions gave us some interesting clues. In our system, the total of DEPE intermolecular hydrogen bonds between the carbonyl and the amine group of the phospholipids decreased from 0.13 per phospholipid in the pure DEPE bilayer to 0.11 per phospholipid in the presence of TMBC. This is interesting because it shows how the catechin alter the intermolecular hydrogen bonding of DEPE bilayer, probably as a consequence of the increase of the area per lipid commented above. In the presence of TMBC, we found that 0.06 new hydrogen bonds per phospholipid were formed between the carbonyl of DEPE and the hydroxyl groups of TMBC, and also 0.05 new hydrogen bonds were formed between the carbonyl group of TMBC and the surrounding water. The total number of hydrogen bonds formed by all the carbonyls groups present in our system did not change in the presence of TMBC, but when we determined the sum of hydrogen bonds plus the total of electrostatic pairs formed at distances shorter than  $3\text{ \AA}$ , we found that they increased from 2.40 per phospholipid for pure DEPE to 2.54 per phospholipid in the presence of TMBC. The

appearance of new hydrogen bonds mediated by TMBC and the increase in the electrostatic interactions with the carbonyl groups of the phospholipid clearly alter the interfacial region of the bilayer, and it might be responsible for the shift of the infrared carbonyl absorption band to lower frequencies as shown above (Fig. 6).

Fig. 7A presents the mass density profile of the simulated bilayer. Some fundamental positions of the DEPE molecule along  $z$ -axis are comprised. The terminal methyl groups to indicate the center of the bilayer (C18 atoms), the position of the double bond in the center of the bilayer (C9 atoms), the carbonyl groups (C1 atoms), the amine group, and the phosphate atoms in the polar head region. TMBC was treated as an all-atom particle, and the mass density profile of TMBC corresponds to the mass distribution of all atoms of the molecule along the  $z$  axis of the membrane. It can be observed that TMBC molecules are mainly located near the carbonyl groups of the phospholipid, extending toward the polar region near the phosphate and amine groups, and also toward the region of the double bond of the phospholipid inside the bilayer, but they almost do not reach the center of the bilayer. This location is interesting because it has been shown that the presence of double bond in the phospholipid acyl chain slowed the *trans-gauche* interconversion, and it produced a pronounced stiffness of the acyl chain near the double bond [57]. The presence of TMBC in this region might be able to perturb this methylene segment and to produce an increase of the *gauche* conformers, in agreement with the increase in the wavenumber of the infrared methylene absorption band shown in Fig. 5. This location is different from that of TMBC in dimyristoylphosphatidylserine bilayers, where TMBC molecules were mainly located in the center of the lipid hydrocarbon chains between the phosphorous atoms and the terminal methyl groups [24]. For saturated phospholipids, the chain conformation and *trans-gauche* isomerism display a characteristic flexibility gradient, with increasing motion towards the terminal methyl end of the acyl chain [58]. A lack of effect on the maximum of the methylene infrared band in this anionic phospholipid was observed [24]. This could be due to the fact that the number of *gauche* isomers in the methylene segments, where TMBC is found, is already high enough not to be altered by the presence of the catechin.

Snapshot of the simulation box of the DEPE/TMBC system is presented in Fig. 7B. It can be seen how TMBC is located in the upper part of the bilayer near the interfacial region of the membrane. This location is in agreement with the experimental and simulated data presented above, TMBC is able to perturb the intermolecular interaction in the polar head of the phospholipid, to increase the area per lipid, to affect the interfacial region of the bilayer, and to disrupt the upper region of the acyl chain palisade increasing the fluidity and decreasing the order of the bilayer.

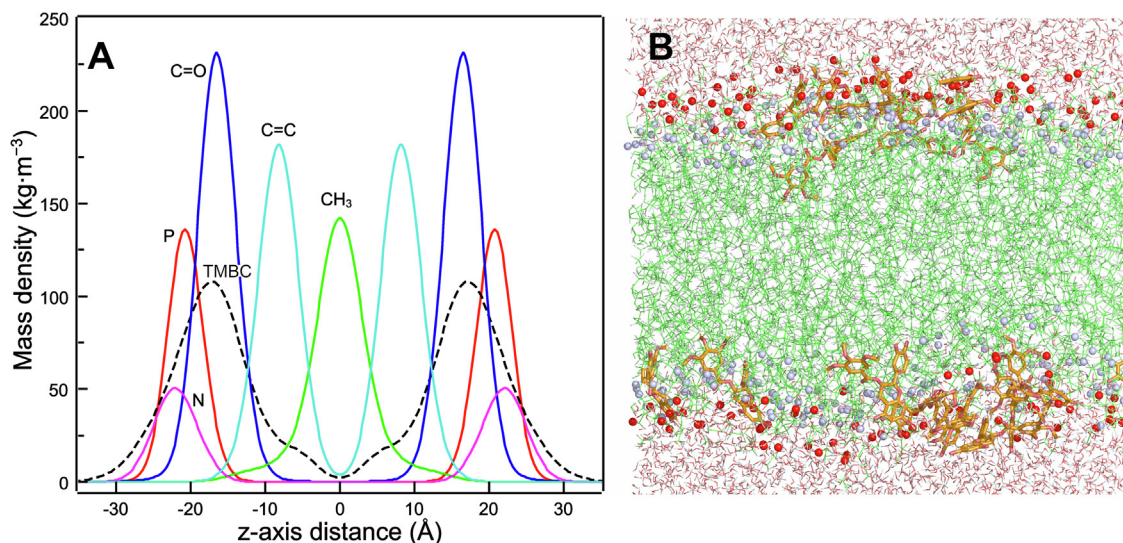


**Fig. 7.** (A) Mass density profiles along the z-axis of the simulation box of DEPE/TMBC membranes at 50 °C. TMBC molecule in dashed black line, and DEPE groups in solid lines marked as follows: P, phosphorus (red); C=O, carbonyl group (dark blue); C=C, double bond (light blue); N, amine group (purple); and CH<sub>3</sub>, terminals methyl carbon atoms (green). (B) Final snapshot of the simulation box of DEPE/TMBC membranes. Water molecules are shown in red lines, TMBC in orange sticks, DEPE in green lines, lipid carbonyl groups in blue spheres, and phosphorous atoms in red spheres.

Fig. 8A shows the propensity of TMBC to aggregate in the bilayer as calculated by the average size of TMBC clusters within a cutoff distance of 3 Å. Less than 10 % of TMBC is found as monomers, the majority of the catechin forms cluster of 2–5 molecules. This is in contrast to the behavior of the molecule in dimyristoylphosphatidylserine bilayers where near 50 % of the catechin molecules were found as monomers [24]. As commented above, this difference might be due to the lower solubility of TMBC in DEPE bilayers when compared to the shorter chain anionic phospholipid. Fig. 8B presents the density map of TMBC in the *x y* plane of the bilayer which exhibits the formation of different cluster along the plane of the bilayer. The presence of these different clusters may reveal the different broad phase transitions observed by DSC (Fig. 2A).

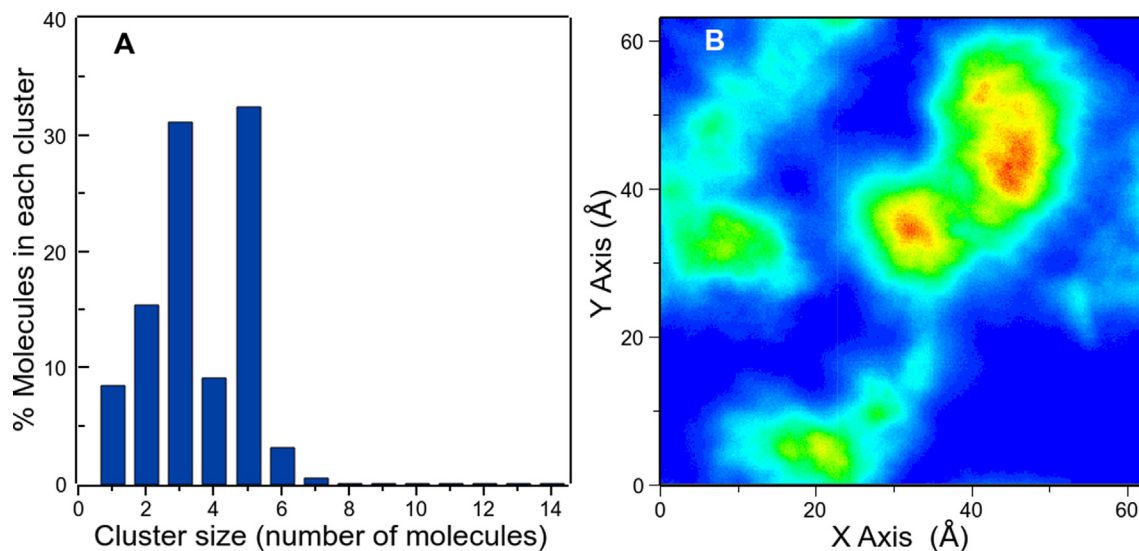
The tendency of DEPE, and other unsaturated phosphatidylethanolamines, to form inverted H<sub>II</sub> phase was early rationalized by the so-called shape-structure concept of lipid polymorphism. A dimensionless number known as the packing parameter was defined as the ratio between the hydrocarbon chain volume and the optimal surface area and the critical acyl chain length [59,60]. The absence of head methyl groups, when compared to phosphatidylcholine, and the strong electrostatic and hydrogen bonding interactions that exist between phosphatidylethanolamine headgroups, both in the plane of the bilayer and between adjacent bilayers, makes the optimal surface area to be small, and then, the packing parameter to be higher than 1. It is this cone-shaped molecule of DEPE which makes it compatible with aggregate structures with a negative curvature like the inverted H<sub>II</sub> phase. We have shown that the presence of TMBC stabilizes the bilayer L $\alpha$  phase blocking the formation of the H<sub>II</sub> phase. The catechin molecule located in the interfacial region of the bilayer, disrupts the intermolecular hydrogen bonding of DEPE, forms new hydrogen bonds with the phospholipid, and increases the area per lipid. These effects would increase the optimal surface area and would decrease the value of the packing parameter. All together, these effects would decrease the negative curvature of the system, and then they would make harder to form the inverted H<sub>II</sub> phase.

A notably intriguing property of the membrane is the distribution of local pressure inside a bilayer, the termed lateral pressure profile. This property is connected to other physical properties of the mem-

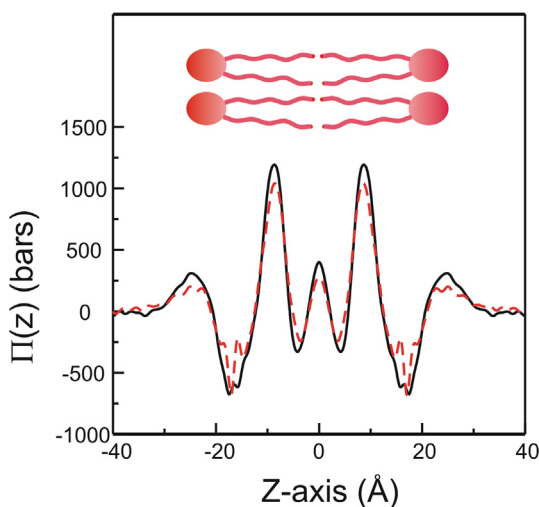
brane like the spontaneous curvature and it is distinctive of the different phospholipid species [61].

Fig. 9 presents the lateral pressure profile across the bilayer for systems composed by pure DEPE and DEPE containing TMBC. The profile corresponding to pure DEPE shows the three different regimes that have been identified in phospholipid bilayers: a repulsive input resulting from hydrophilic head groups as a result of electrostatic and steric interactions and hydration repulsion; and attractive input as a result of the interfacial energy between the water and the hydrocarbon phase, attempting to minimize the surface area; and a repulsive input as a result of the hydrophobic chains due to steric interactions [62]. The presence of an additional peak in the center of the bilayer has been suggested to emerge from interdigitation of the two monolayers [63]. As it has been proposed previously, conical-shaped nonbilayer lipids like DEPE show an increase in the lateral pressure in the acyl chain region, and a decrease in the lateral pressure among the lipid headgroups [64].

As can be seen in Fig. 9, the presence of TMBC alters the lateral pressure profile appreciably, the catechin reduces the magnitude of the pressure of all the peaks. We showed above that TMBC decreases the thickness of the bilayer, and this might be the reason why the profile in the presence of TMBC is moderately narrower and accordingly the peaks relocate toward the center of the bilayer. The prominent positive peak at the membrane water interface is markedly decreased, and this can be related to the observed breaking of the intermolecular hydrogen bonds between the carbonyl and amino groups of DEPE and the screening of the electrostatic interactions between the head groups. This influence is complemented by the detected increase in area per lipid in the presence of TMBC. The decrease of the evident negative peak closer to the membrane interior around the carbonyl region can be attributed to the location of TMBC at the border between the hydrophobic and hydrophilic regions of the bilayer, the presence of TMBC in this part of the bilayer could reduce the hydrophobic effect. This behavior is similar to the one previously described for alcohols on lipid membranes, the alterations due to alcohols were plainly localized to the area under the lipid head groups, which is the region where alcohols are located [65]. These effects on the interfacial region of the bilayer contribute to the stabilization of the L $\alpha$  phase toward the inverted phase formation in DEPE system, which is an already



**Fig. 8.** (A) Cluster size distribution of TMBC molecules in the DEPE membrane. (B) Density map of TMBC molecules of the DEPE/TMBC membrane corresponding to the x y plane of the simulation box. TMBC density increases from blue to red color.



**Fig. 9.** Lateral pressure profiles,  $\Pi(z)$ , across the membrane for pure DEPE (solid black line) and DEPE/TMBC (dashed red line) bilayers. The membrane center is at  $z = 0$  along the membrane normal direction.

known effect of alcohols [66,67]. However, the location of TMBC in the bilayer extends to the acyl chain palisade, and then the effect of TMBC is more extensive than that of the alcohols; while the alcohols had almost no effect in the central part of the membrane [68], it is clear from Fig. 9 that TMBC also decreases the positive peak due to the repulsion between the hydrocarbon chains in the center region of the bilayer. This considerable alteration of the lateral pressure profile is important as it has been implicated in the modulation of biological phenomena, including binding and properties of membrane protein [69–71].

#### 4. Conclusions

Catechins show a wide variety of beneficial effects for health, highlighting among them their anticancer effects. The biological activity of catechins is known to affect membrane-dependent cellular processes, and an important strategy to enhance their membrane interaction is the structural modification of the catechin

molecule. There is significant evidence that the physical properties of lipids contribute to membrane function by modulating the organization and distribution of membrane proteins. In this context, it is crucial to know how semisynthetic catechin TMBC affects these membrane properties. In this work we have studied in detail the molecular interaction between TMBC and biomimetic membranes formed by DEPE. Through the use of various biophysical techniques (DSC, FTIR, X-ray diffraction) and molecular dynamics simulation, we have obtained information about the effect of TMBC on important physical properties of the lipid bilayer such as fluidity, bilayer thickness, hydrogen bonding, domain formation, and lateral pressure profile across the lipid bilayer. The information obtained has allowed us to know the effect of TMBC on lipid polymorphism, an important aspect of membrane properties that until now had not been studied. TMBC is easily incorporated into the DEPE bilayers where it considerably alters the physical properties of the phospholipid. In some cases, this alteration is different from those exerted on bilayers composed of another class of phospholipids. TMBC shifts the phase transition from  $L\beta$  to  $L\alpha$  to lower temperatures and produces immiscibility in this gel phase. In the liquid crystalline phase, TMBC decreases the thickness of the bilayer and alters the interfacial region of the membrane. An important effect is that TMBC is able to prevent the formation of the  $H_{II}$  phase and stabilize the  $L\alpha$  phase. Computer simulation data were supported by those obtained experimentally. Molecular dynamics simulations showed that TMBC forms clusters at the top of the phospholipid palisade that modify the lateral pressure profile of the bilayer, and it explains the ability of TMBC to stabilize the lamellar  $L\alpha$  phase. The ability of this modified catechin to prevent the formation of the inverted hexagonal phase is relevant because it is known that lipids with a tendency to form non-lamellar phases are very important in the modulation of protein activity and therefore in the regulation of membrane function. We believe that these results might help to understand the mechanism of the interaction of TMBC with the membrane in its antitumor role and also in other membrane related biological actions of catechins.

#### CRediT authorship contribution statement

**Elisa Aranda:** Investigation, Visualization. **José A. Teruel:** Software, Formal analysis. **Antonio Ortiz:** Validation, Resources. **María**

**Dolores Pérez-Cárceles:** Conceptualization, Resources. **J. Neptuno Rodríguez-López:** Funding acquisition, Resources. **Francisco J. Aranda:** Supervision, Writing – review & editing.

## Data availability

No data was used for the research described in the article.

## Declaration of Competing Interest

The authors declare that they have no known competing financial interests or personal relationships that could have appeared to influence the work reported in this paper.

## Acknowledgments

The Computational Service of the University de Murcia (Spain) is acknowledged for the allocated computational time on its supercomputing facilities.

## Funding

This research was funded by a grant from the Fundación Séneca, Región de Murcia, Spain (FS-RM) (20809/PI/18). The funding source had no involvement in study design, in the collection, analysis and interpretation of data, in the writing of the report, and in the decision to submit the article for publication.

## References

- [1] B.N. Singh, S. Shankar, R.K. Srivastava, Green tea catechin, epigallocatechin-3-gallate (EGCG): Mechanisms, perspectives and clinical applications, *Biochem. Pharmacol.* 82 (2011) 1807–1821, <https://doi.org/10.1016/j.bcp.2011.07.093>.
- [2] H. Fujiki, E. Sueoka, T. Watanabe, M. Suganuma, Synergistic enhancement of anticancer effects on numerous human cancer cell lines treated with the combination of EGCG, other green tea catechins, and anticancer compounds, *J. Cancer Res. Clin. Oncol.* 141 (2015) 1511–1522, <https://doi.org/10.1007/s00432-014-1899-5>.
- [3] A. Negri, V. Naponelli, F. Rizzi, S. Bettuzzi, Molecular targets of epigallocatechin-gallate (EGCG): A special focus on signal transduction and cancer, *Nutrients*. 10 (12) (2018) 1936, <https://doi.org/10.3390/nu10121936>.
- [4] N. Caturla, E. Vera-Samper, J. Villalán, C.R. Mateo, V. Micol, The relationship between the antioxidant and the antibacterial properties of galloylated catechins and the structure of phospholipid model membranes, *Free Radic. Biol. Med.* 34 (2003) 648–662, [https://doi.org/10.1016/S0891-5849\(02\)01366-7](https://doi.org/10.1016/S0891-5849(02)01366-7).
- [5] T. Watanabe, H. Kuramochi, A. Takahashi, K. Imai, N. Katsuta, T. Nakayama, H. Fujiki, M. Suganuma, Higher cell stiffness indicating lower metastatic potential in B16 melanoma cell variants and in (2)-epigallocatechin gallate-treated cells, *J. Cancer Res. Clin. Oncol.* 138 (2012) 859–866, <https://doi.org/10.1007/s00432-012-1159-5>.
- [6] A. Takahashi, T. Watanabe, A. Mondal, K. Suzuki, M. Kurusu-Kanno, Z. Li, T. Yamazaki, H. Fujiki, M. Suganuma, Mechanism-based inhibition of cancer metastasis with (-)-epigallocatechin gallate, *Biochem. Biophys. Res. Commun.* 443 (2014) 1–6, <https://doi.org/10.1016/j.bbrc.2013.10.094>.
- [7] D. Duhon, R.L.H. Bigelow, D.T. Coleman, J.J. Steffan, C. Yu, W. Langston, C.G. Kevil, J.A. Cardelli, The polyphenol epigallocatechin-3-gallate affects lipid rafts to block activation of the c-Met receptor in prostate cancer cells, *Mol. Carcinog.* 49 (2010) 739–749, <https://doi.org/10.1002/mc.20649>.
- [8] G. van Meer, D.R. Voelker, G.W. Feigenson, Membrane lipids: where they are and how they behave, *Nat Rev Mol Cell Biol.* 9 (2008) 112–124, <https://doi.org/10.1038/nrm2330>.
- [9] J.E. Vance, Phosphatidylserine and phosphatidylethanolamine in mammalian cells: Two metabolically related aminophospholipids, *J. Lipid Res.* 49 (2008) 1377–1387, <https://doi.org/10.1194/jlr.R700020-JLR200>.
- [10] E. Calzada, O. Onguka, S.M. Claypool, Phosphatidylethanolamine Metabolism in Health and Disease, *Int. Rev. Cell Mol. Biol.* 321 (2016) 29–88, <https://doi.org/10.1016/bs.ircmb.2015.10.001>.
- [11] A. Chakrabarti, Phospholipid Asymmetry in Biological Membranes: Is the Role of Phosphatidylethanolamine Underappreciated?, *J. Membr. Biol.* 254 (2021) 127–132, <https://doi.org/10.1007/s00232-020-00163-w>.
- [12] T. Harayama, H. Riezman, Understanding the diversity of membrane lipid composition, *Nat. Rev. Mol. Cell Biol.* 19 (2018) 281–296, <https://doi.org/10.1038/nrm.2017.138>.
- [13] W. Dowhan, M. Bogdanov, Lipid-Dependent Membrane Protein Topogenesis, *Annu Rev Biochem.* 78 (1) (2009) 515–540, <https://doi.org/10.1146/annurev.biochem.77.060806.091251>.
- [14] J.H. Stafford, P.E. Thorpe, Increased exposure of phosphatidylethanolamine on the surface of tumor vascular endothelium, *Neoplasia*. 13 (2011) 299–308, <https://doi.org/10.1593/neo.101366>.
- [15] L.T.H. Tan, K.G. Chan, P. Pusparajah, W.L. Lee, L.H. Chuah, T.M. Khan, L.H. Lee, B. H. Goh, Targeting membrane lipid a potential cancer cure?, *Front Pharmacol.* 8 (2017) 1–6, <https://doi.org/10.3389/fphar.2017.00012>.
- [16] S. Troeira Henriques, Y.H. Huang, S. Chaousis, C.K. Wang, D.J. Craik, Anticancer and toxic properties of cyclotides are dependent on phosphatidylethanolamine phospholipid targeting, *ChemBioChem* 15 (2014) 1956–1965, <https://doi.org/10.1002/cbic.201402144>.
- [17] C. Chidley, S.A. Trauger, K. Birsoy, E.K. O'Shea, The anticancer natural product ophiobolin A induces cytotoxicity by covalent modification of phosphatidylethanolamine, *Elife*. 5 (2016) 1–20, <https://doi.org/10.7554/eLife.14601>.
- [18] D. Patel, S.N. Witt, Ethanolamine and Phosphatidylethanolamine: Partners in Health and Disease, *Oxid. Med. Cell. Longev.* 2017 (2017) 1–18, <https://doi.org/10.1155/2017/4829180>.
- [19] J. Hong, H. Lu, X. Meng, J.H. Ryu, Y. Hara, C.S. Yang, Stability, cellular uptake, biotransformation, and efflux of tea polyphenol (-)-epigallocatechin-3-gallate in HT-29 human colon adenocarcinoma cells, *Cancer Res.* 62 (2002) 7241–7246.
- [20] M. Sáez-Ayala, L. Sánchez-Del-Campo, M.F. Montenegro, S. Chazarra, A. Tárrega, J. Cabezas-Herrera, J.N. Rodríguez-López, Comparison of a Pair of Synthetic Tea-Catechin-Derived Epimers: Synthesis, Antifolate Activity, and Tyrosinase-Mediated Activation in Melanoma, *Chem. Med. Chem.* 6 (2011) 440–449, <https://doi.org/10.1002/cmdc.201000482>.
- [21] M.F. Montenegro, M. Sáez-Ayala, A. Piñero-Madrona, J. Cabezas-Herrera, J.N. Rodríguez-López, J.Q. Cheng, Reactivation of the Tumour Suppressor RASSF1A in Breast Cancer by Simultaneous Targeting of DNA and E2F1 Methylation, *PLoS ONE* 7 (12) (2012) e52231, <https://doi.org/10.1371/journal.pone.0052231>.
- [22] C.W. How, J.A. Teruel, A. Ortiz, M.F. Montenegro, J.N. Rodríguez-López, F.J. Aranda, Effects of a synthetic antitumoral catechin and its tyrosinase-processed product on the structural properties of phosphatidylcholine membranes, *Biochim. Biophys. Acta - Biomembr.* 2014 (1838) 1215–1224, <https://doi.org/10.1016/j.bbamem.2014.01.025>.
- [23] F. Casado, J.A. Teruel, S. Casado, A. Ortiz, J.N. Rodríguez-López, F. Aranda, Location and effects of an antitumoral catechin on the structural properties of phosphatidylethanolamine membranes, *Molecules* 21 (7) (2016) 829, <https://doi.org/10.3390/molecules21070829>.
- [24] E. Aranda, J.A. Teruel, A. Ortiz, M.D. Pérez-Cárceles, J.N. Rodríguez-López, F.J. Aranda, 3,4,5-Trimethoxybenzoate of Catechin, an Anticarcinogenic Semisynthetic Catechin, Modulates the Physical Properties of Anionic Phospholipid Membranes, *Molecules* 27 (2022) 1–16, <https://doi.org/10.3390/molecules27092910>.
- [25] C.J.F. Böttcher, C.M. Van gent, C. Pries, C. Gent, C. Pries, A rapid and sensitive sub-micro phosphorus determination, *Anal. Chim. Acta.* 24 (1961) 203–204.
- [26] S. Kim, P.A. Thiessen, E.E. Bolton, J. Chen, G. Fu, A. Gindulyte, L. Han, J. He, S. He, B.A. Shoemaker, J. Wang, B. Yu, J. Zhang, S.H. Bryant, PubChem substance and compound databases, *Nucleic Acids Res.* 44 (2016) D1202–D1213, <https://doi.org/10.1093/nar/gkv951>.
- [27] M.J. Abraham, T. Murtola, R. Schulz, S. Páll, J.C. Smith, B. Hess, E. Lindahl, Gromacs: High performance molecular simulations through multi-level parallelism from laptops to supercomputers, *SoftwareX*. 1–2 (2015) 19–25, <https://doi.org/10.1016/j.softx.2015.06.001>.
- [28] S. Jo, T. Kim, V.G. Iyer, W. Im, CHARMM-GUI: A Web-Based Graphical User Interface for CHARMM, *J. Comput. Chem.* 29 (2008) 1859–1865.
- [29] B.R. Brooks, C.L. Brooks, A.D. Mackerell, L. Nilsson, R.J. Petrella, B. Roux, Y. Won, G. Archontis, C. Bartels, S. Boresch, A. Caffisch, L. Caves, Q. Cui, A.R. Dinner, M. Feig, S. Fischer, J. Gao, M. Hodoscek, W. Im, K. Kuczera, T. Lazaridis, J. Ma, V. Ovchinnikov, E. Paci, R.W. Pastor, C.B. Post, J.Z. Pu, M. Schaefer, B. Tidor, R.M. Venable, H.L. Woodcock, X. Wu, W. Yang, D.M. York, M. Karplus, CHARMM: The biomolecular simulation program, *J. Comput. Chem.* 30 (10) (2009) 1545–1614.
- [30] J. Lee, X.i. Cheng, J.M. Swails, M.S. Yeom, P.K. Eastman, J.A. Lemkul, S. Wei, J. Buckner, J.C. Jeong, Y. Qi, S. Jo, V.S. Pande, D.A. Case, C.L. Brooks, A.D. Mackerell, J.B. Klauda, W. Im, CHARMM-GUI Input Generator for NAMD, GROMACS, AMBER, OpenMM, and CHARMM/OpenMM Simulations Using the CHARMM36 Additive Force Field, *J. Chem. Theory Comput.* 12 (1) (2016) 405–413.
- [31] L. Martínez, R. Andrade, E.G. Birgin, J.M. Martínez, PACKMOL: A Package for Building Initial Configurations for Molecular Dynamics Simulations, *J. Comput. Chem.* 30 (2009) 2157–2164.
- [32] H.J.C. Berendsen, J.P.M. Postma, W.F. Van Gunsteren, A. Dinola, J.R. Haak, Molecular dynamics with coupling to an external bath, *J. Chem. Phys.* 81 (1984) 3684–3690, <https://doi.org/10.1063/1.448118>.
- [33] W.G. Hoover, Canonical Dynamics: Equilibrium Phase-Space Distributions, *Phys. Rev. A*. 31 (1985) 1695–1697.
- [34] M. Parrinello, A. Rahman, Polymorphic transitions in single crystals: A new molecular dynamics method, *J. Appl. Phys.* 52 (1981) 7182–7190, <https://doi.org/10.1063/1.328693>.
- [35] L. Schrödinger, The PyMOL Molecular Graphics System, Version 2 (2010) 3.
- [36] O.H.S. Ollila, H.J. Risselada, M. Louhivuori, E. Lindahl, I. Vattulainen, S.J. Marrink, 3D Pressure field in lipid membranes and membrane-protein

- complexes, *Phys. Rev. Lett.* 102 (2009) 1–4, <https://doi.org/10.1103/PhysRevLett.102.078101>.
- [37] R.C. Snoeberger III, T. Lian, V.S. Batista, The influence of surface hydration on the interfacial electron transfer dynamics from Rhodamine B into SnO<sub>2</sub>, *Phys. Chem. Interfaces Nanomater.* VIII. 7396 (2009), <https://doi.org/10.1117/12.829483>.
- [38] J.M. Vanegas, A. Torres-Sánchez, M. Arroyo, Importance of force decomposition for local stress calculations in biomembrane molecular simulations, *J. Chem. Theory Comput.* 10 (2014) 691–702, <https://doi.org/10.1021/ct4008926>.
- [39] A. Torres-Sánchez, J.M. Vanegas, M. Arroyo, Examining the mechanical equilibrium of microscopic stresses in molecular simulations, *Phys. Rev. Lett.* 114 (2015) 1–5, <https://doi.org/10.1103/PhysRevLett.114.258102>.
- [40] J.A. Killian, B. de Kruijff, Thermodynamic, Motional, and Structural Aspects of Gramicidin-Induced Hexagonal HII Phase Formation in Phosphatidylethanolamine, *Biochemistry* 24 (1985) 7881–7890, <https://doi.org/10.1021/bi00348a006>.
- [41] J.J. Chicano, A. Ortiz, J.A. Teruel, F.J. Aranda, Organotin compounds promote the formation of non-lamellar phases in phosphatidylethanolamine membranes, *Biochim. Biophys. Acta - Biomembr.* 1558 (2002) 70–81, [https://doi.org/10.1016/S0005-2736\(01\)00426-6](https://doi.org/10.1016/S0005-2736(01)00426-6).
- [42] V. Luzzati, X-ray diffraction studies of lipid-water systems, in: D. Chapman (Ed.), *Biol. Membr.*, Academic Press, New York, 1968; pp. 71–123.
- [43] A. Ortiz, J.A. Teruel, M.J. Espuny, A. Marqués, Á. Manresa, F.J. Aranda, Interactions of a Rhodococcus sp. biosurfactant trehalose lipid with phosphatidylethanolamine membranes, *Biochim. Biophys. Acta - Biomembr.* 1778 (12) (2008) 2806–2813, <https://doi.org/10.1016/j.bbamem.2008.07.016>.
- [44] A. Cordero, J. Prades, J. Frau, O. Vögler, S.S. Funari, J.J. Perez, P.V. Escibá, F. Barceló, Interactions of fatty acids with phosphatidylethanolamine membranes: X-ray diffraction and molecular dynamics studies, *J. Lipid Res.* 51 (2010) 1113–1124, <https://doi.org/10.1194/jlr.M003012>.
- [45] C. Valtersson, G. van Duyn, A.J. Verkleij, T. Chojnacki, B. de Kruijff, G. Dallner, The influence of dolichol, dolichol esters, and dolichyl phosphate on phospholipid polymorphism and fluidity in model membranes, *J. Biol. Chem.* 260 (1985) 2742–2751, [https://doi.org/10.1016/s0021-9258\(18\)89424-8](https://doi.org/10.1016/s0021-9258(18)89424-8).
- [46] J.A. Killian, C.W. van den Berg, H. Tournois, S. Keur, A.J. Slotboom, G.J.M. van Scharrenburg, B. de Kruijff, Gramicidin-induced hexagonal HII phase formation in negatively charged phospholipids and the effect of N- and C-terminal modification of gramicidin on its interaction with zwitterionic phospholipids, *BBA - Biomembr.* 857 (1986) 13–27, [https://doi.org/10.1016/0005-2736\(86\)90094-5](https://doi.org/10.1016/0005-2736(86)90094-5).
- [47] L. Zhao, S.S. Feng, Effects of lipid chain length on molecular interactions between paclitaxel and phospholipid within model biomembranes, *J. Colloid Interface Sci.* 274 (2004) 55–68, <https://doi.org/10.1016/j.jcis.2003.12.009>.
- [48] M.M.G. Krishna, N. Periasamy, Location and orientation of DODCI in lipid bilayer membranes: Effects of lipid chain length and unsaturation, *Biochim. Biophys. Acta - Biomembr.* 1461 (1999) 58–68, [https://doi.org/10.1016/S0005-2736\(99\)00149-2](https://doi.org/10.1016/S0005-2736(99)00149-2).
- [49] R. Mendelsohn, H.H. Mantsch, *Fourier transform infrared studies of lipid-protein interactions*, in: A. Watts, J.J.H.M. De Pont (Eds.), *Progress in Lipid Protein Interaction*, Elsevier, New York, 1986, pp. 103–146.
- [50] H.H. Mantsch, A. Martin, D.G. Cameron, Characterization by Infrared Spectroscopy of the Bilayer to Nonbilayer Phase Transition of Phosphatidylethanolamines, *Biochemistry* 20 (1981) 3138–3145, <https://doi.org/10.1021/bi00514a024>.
- [51] A. Blume, W. Huebner, G. Messner, Fourier Transform Infrared Spectroscopy of 13C:0 labeled Phospholipids Hydrogen Bonding To Carbonyl Groups, *Biochemistry* 27 (1988) 8239–8249, <https://doi.org/10.1021/bi00421a038>.
- [52] R.N.A.H. Lewis, R.N. McElhane, Calorimetric and spectroscopic studies of the polymorphic phase behavior of a homologous series of n-saturated 1,2-diacyl phosphatidylethanolamines, *Biophys. J.* 64 (1993) 1081–1096, [https://doi.org/10.1016/S0006-3495\(93\)81474-7](https://doi.org/10.1016/S0006-3495(93)81474-7).
- [53] J. Castresana, J.L. Nieva, E. Rivas, A. Alonso, Partial dehydration of phosphatidylethanolamine phosphate groups during hexagonal phase formation, as seen by i.r. spectroscopy, *Biochem. J.* 282 (1992) 467–470, <https://doi.org/10.1042/bj2820467>.
- [54] J. Katsaras, D.S.C. Yang, R.M. Epand, K.R. Jeffrey, Direct Evidence for the Partial Dehydration of Phosphatidylethanolamine Bilayers on Approaching the Hexagonal Phase, *Biochemistry* 32 (1993) 10700–10707, <https://doi.org/10.1021/bi00091a021>.
- [55] J.A. Killian, Hydrophobic mismatch between proteins and lipids in membranes, *Biochim. Biophys. Acta - Rev. Biomembr.* 1376 (1998) 401–416, [https://doi.org/10.1016/S0304-4157\(98\)00017-3](https://doi.org/10.1016/S0304-4157(98)00017-3).
- [56] L.E. Cybulski, D. de Mendoza, Bilayer Hydrophobic Thickness and Integral Membrane Protein Function, *Curr. Protein Pept. Sci.* 12 (2011) 760–766, <https://doi.org/10.2174/138920311798841681>.
- [57] L.A. Dalton, K.W. Miller, Trans-unsaturated lipid dynamics: modulation of dielaidoylphosphatidylcholine acyl chain motion by ethanol, *Biophys. J.* 65 (1993) 1620–1631, [https://doi.org/10.1016/S0006-3495\(93\)81207-4](https://doi.org/10.1016/S0006-3495(93)81207-4).
- [58] M. Moser, D. Marsh, P. Meier, K.H. Wassmer, G. Kothe, Chain configuration and flexibility gradient in phospholipid membranes. Comparison between spin-label electron spin resonance and deuterium nuclear magnetic resonance, and identification of new conformations, *Biophys. J.* 55 (1989) 111–123, [https://doi.org/10.1016/S0006-3495\(89\)82784-5](https://doi.org/10.1016/S0006-3495(89)82784-5).
- [59] J.N. Israelachvili, *Intermolecular and Surface Forces*, Academic Press (2011), <https://doi.org/10.1016/C2009-0-21560-1>.
- [60] V.A. Frolov, A.V. Shnyrova, J. Zimmerberg, Lipid polymorphisms and membrane shape, *Cold Spring Harb. Perspect. Biol.* 3 (11) (2011) a004747–a.
- [61] W. Ding, M. Palaiokostas, W. Wang, M. Orsi, Effects of Lipid Composition on Bilayer Membranes Quantified by All-Atom Molecular Dynamics, *J. Phys. Chem. B.* 119 (2015) 15263–15274, <https://doi.org/10.1021/acs.jpcc.5b06604>.
- [62] S. Ollila, M.T. Hyvönen, I. Vattulainen, Polyunsaturation in lipid membranes: Dynamic properties and lateral pressure profiles, *J. Phys. Chem. B.* 111 (2007) 3139–3150, <https://doi.org/10.1021/jp065424f>.
- [63] E. Van Den Brink-Van Der Laan, J.A. Killian, B. De Kruijff, Nonbilayer lipids affect peripheral and integral membrane proteins via changes in the lateral pressure profile, *Biochim. Biophys. Acta - Biomembr.* 1666 (2004) 275–288, <https://doi.org/10.1016/j.bbamem.2004.06.010>.
- [64] S.M. Bezrukov, Functional consequences of lipid packing stress, *Curr. Opin. Colloid Interface Sci.* 5 (2000) 237–243, [https://doi.org/10.1016/S1359-0294\(00\)00061-3](https://doi.org/10.1016/S1359-0294(00)00061-3).
- [65] E. Terama, O.H.S. Ollila, E. Salonen, A.C. Rowat, C. Trandum, P. Westh, M. Patra, M. Karttunen, I. Vattulainen, Influence of ethanol on lipid membranes: From lateral pressure profiles to dynamics and partitioning, *J. Phys. Chem. B.* 112 (2008) 4131–4139, <https://doi.org/10.1021/jp0750811>.
- [66] J.A. Veiro, R.G. Khalifah, E.S. Rowe, The polymorphic phase behavior of dielaidoylphosphatidylethanolamine, Effect of n-alkanols, *BBA - Biomembr.* 979 (1989) 251–256, [https://doi.org/10.1016/0005-2736\(89\)90441-0](https://doi.org/10.1016/0005-2736(89)90441-0).
- [67] P. Urbina, A. Alonso, F.X. Contreras, F.M. Goñi, D.J. López, L.R. Montes, J. Sot, Alkanes are not innocuous vehicles for hydrophobic reagents in membrane studies, *Chem. Phys. Lipids.* 139 (2006) 107–114, <https://doi.org/10.1016/j.chemphyslip.2005.11.002>.
- [68] A.L. Frischknecht, L.J.D. Frink, Alcohols reduce lateral membrane pressures: Predictions from molecular theory, *Biophys. J.* 91 (2006) 4081–4090, <https://doi.org/10.1529/biophysj.106.091918>.
- [69] D. Marsh, Lateral pressure profile, spontaneous curvature frustration, and the incorporation and conformation of proteins in membranes, *Biophys. J.* 93 (2007) 3884–3899, <https://doi.org/10.1529/biophysj.107.107938>.
- [70] K. Corin, J.U. Bowie, How bilayer properties influence membrane protein folding, *Protein Sci.* 29 (2020) 2348–2362, <https://doi.org/10.1002/pro.3973>.
- [71] J.C. Bozelli, S.S. Aulakh, R.M. Epand, Membrane shape as determinant of protein properties, *Biophys. Chem.* 273 (2021) 106587.